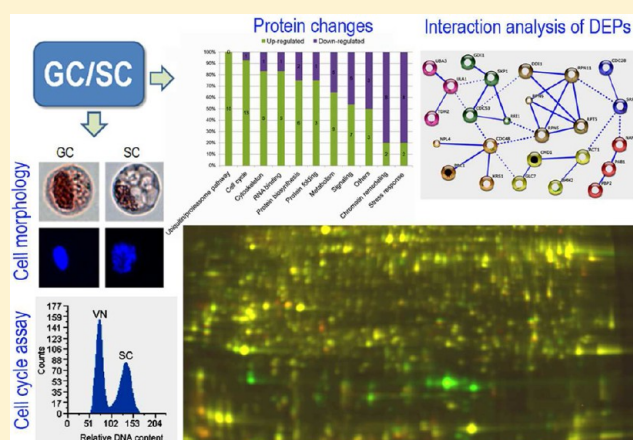


Comparative Proteomic Analysis of Generative and Sperm Cells Reveals Molecular Characteristics Associated with Sperm Development and Function Specialization

Xin Zhao,^{†,‡} Ning Yang,^{†,‡} and Tai Wang^{*,†}[†]Key Laboratory of Plant Molecular Physiology, Institute of Botany, Chinese Academy of Sciences and National Center for Plant Gene Research, Beijing 100093, China[‡]University of Chinese Academy of Sciences, Beijing 100049, China**S** Supporting Information

ABSTRACT: In flowering plants, two sperm cells (SCs) are generated from a generative cell (GC) in the developing pollen grain or growing pollen tube and are then delivered to the embryo sac to initiate double fertilization. SC development and function specialization involve the strict control of the protein (gene) expression program and coordination of diverse cellular processes. However, because methods for collecting a large amount of highly purified GCs and SCs for proteomic and transcriptomic studies from a plant are not available, molecular information about the program and the interconnections is lacking. Here, we describe a method for obtaining a large quantity of highly purified GCs and SCs from just-germinated lily pollen grains and growing pollen tubes for proteomic analysis. Our observation showed that SCs had less condensed chromatin and more vacuole-like structures than GCs and that mature SCs were arrested at the G2 phase. Comparison of SC and GC proteomes revealed 101 proteins differentially expressed in the two proteomes. These proteins are involved in diverse cellular and metabolic processes, with preferential involvement in metabolism, the cell cycle, signaling, the ubiquitin/proteasome pathway, and chromatin remodeling. Impressively, almost all proteins in SCF complex-mediated proteolysis and the cell cycle were up-regulated in SCs, whereas those in chromatin remodeling and stress response were down-regulated. Our data also reveal the coordination of SCF complex-mediated proteolysis, cell cycle progression, and DNA repair in SC development and function specialization. This study revealed for the first time a difference in protein profiles between GCs and SCs.

KEYWORDS: comparative proteomics, proteins, pollen grains, pollen tubes, generative cells, sperm cells

**INTRODUCTION**

Sexual plant reproduction is greatly important to mankind. During this process, male gametophytes (pollen grains) play a vital role in plant fertility and crop production through generating and delivering sperm cells (SCs) to the embryo sac for double fertilization, finally giving rise to seeds, which are an important food source for humans and livestock. Understanding the molecular mechanism of pollen and SC development is essential to manipulation of male fertility for plant breeding and heterosis utilization. In flowering plants, pollen develops within anthers, the specialized male reproductive organs.^{1–3} Pollen mother cells in anthers produce haploid unicellular microspores. Subsequently, a microspore undergoes asymmetric mitosis (pollen mitosis I; PMI) to generate a large vegetative cell and a small generative cell (GC) embedded in the vegetative cell. The vegetative cell is fate-determined, whereas the GC further enters a symmetric mitosis (pollen mitosis II; PMII) to produce twin SCs. The place and time of

PMII depend on the species. In some plants, such as *Arabidopsis* and rice, PMII occurs in developing pollen, and the mature pollen is tricellular, whereas in plants such as lily and tobacco, PMII occurs in polarly growing pollen tubes after pollination, and the mature pollen is bicellular at anthesis.^{1–3}

As direct participants in plant fertilization and carrier of genetic information, SCs develop under strict control to ensure their genetic stability and ability for successful fertilization. Although they have several morphological features similar to GCs, SCs differ from GCs in some aspects. SCs are terminally differentiated, can undergo DNA replication before pollination and fertilization, and are usually arrested at the G1 or G2 phase at maturity in different species.⁴ These features suggest that SC

Special Issue: Agricultural and Environmental Proteomics

Received: April 1, 2013

Published: July 24, 2013

development involves subtle control of the cell cycle to avoid genome aneuploidy. The specialized function of SCs also requires a mechanism for DNA damage repair and chromatin condensation, which involves alternation of histone variants and modification.⁵ Recent studies identified genes implicated in SC development and function mainly in *Arabidopsis*. Examples are *CDKA;1*, *FBL17*, *DUO1*, *DUO2*, *AtGEX1*, and *HAP2*, from *Arabidopsis*.^{6–10} Mutation in *CDKA;1*, *FBL17*, *DUO1* and *DUO2* led to defects in PMII; thus, the mature pollen was bicellular. The first two mutants had an SC-like “GC” with about 1.4C DNA content that could fertilize the egg cell, whereas the latter two had a GC-like “GC” with about 2C DNA content that was unable to fertilize. These lines of evidence strongly suggest that the development program from GCs to SCs is essential for SC function specification for fertilization. *AtGEX1* and *HAP2* encode membrane-associated proteins specific to SCs in *Arabidopsis* (though *HAP2* is a homologue of lily *GCS1* which is enriched in both GCs and SCs in lily); mutation in the two genes led to defects in recognition or membrane fusion of SCs with female gametes and embryo lethality.^{9,10} Although cellular features of SC development are well-known and several studies have identified genes involved in SC development and function, the involved molecular mechanism remains unclear.

Recent transcriptomic studies of SCs from rice and *Arabidopsis* showed that the transcriptome of SC significantly differs from that of pollen grains and sporophytic tissues and also revealed a set of sperm-preferential transcripts. These transcripts were overrepresented by transcripts involved in DNA repair, the ubiquitin/proteasome system, cell cycle progression, and epigenetic regulation.^{11,12} Small RNA-mediated DNA methylation in *Arabidopsis* sperms was found associated with epigenetic inheritance, transposon silencing, and paternal imprinting.¹³ These results provide novel insights into the genetic and epigenetic mechanism underlying SC function specialization and are important to decipher the mechanism by biological function analysis of these sperm-expressed genes. Further systematic “omics” analysis of molecular programs involved in SC generation from GCs are essential to understand the molecular regulation underlying SC development and function specialization. The proteome of mature and germinated pollen tubes has been widely studied in various species.^{14–18} However, because the SC generation from GCs involves a short time window in vivo in rice and *Arabidopsis*¹ and isolating GCs from developing pollen is difficult, the molecular program is still unknown.

Lily pollen is bicellular at anthesis, and SCs are generated in polarly growing pollen tubes. This feature provides a possibility to isolate GCs and SCs using pollen grains and pollen tubes, respectively. Furthermore, in vitro-cultured lily pollen tubes grow long enough to allow cytological observation of the tube.¹⁹ Thus, pollen has been one of the best model systems for studying the mechanism of polar growth of pollen tubes and for investigating molecular signatures of GCs.^{19,20} Studies of pollen also lead to identification of the important genes *LGCI* and *GCS1*, which is essential for angiosperm fertilization^{21,22} and histone variants gH3, gCH2A, and soH3-1 expressed specifically in GCs and SCs.^{23,24} In this study, we optimized germination conditions to allow pollen tubes to grow in vitro for a long time with SCs generated in the tubes and established a procedure for obtaining a large amount of highly purified GCs and SCs from just-germinated pollen grains and pollen tubes, respectively. Using these cells, we analyzed protein expression profiles of

GCs and SCs and identified 101 differentially expressed proteins between the two proteomes using 2D-differential in-gel electrophoresis (2D-DIGE) and spectrometry. These proteins are involved in 11 functional groups with a skew toward signaling, the ubiquitin/proteasome pathway, cell cycle control, and chromatin remodeling. Proteins in ubiquitin/proteasome pathway were the main components of the SCF E3 ligase-mediated ubiquitin/proteasome proteolysis pathway and displayed interaction with those involved in GTPase signaling, the cell cycle, and DNA repair.

■ MATERIALS AND METHODS

Isolation of GCs and SCs

Mature pollen grains (MPGs) at anthesis collected from the Lanzhou lily (*Lilium davidii* var. *unicolor*) were dried briefly at room temperature and stored at -20°C . For in vitro germination, stored MPGs were prehydrated in a moisture-saturated chamber at 4°C for 4 to 6 h, then washed with 15% sucrose solution to remove the lipid materials wrapping the pollen grains. These pretreated MPGs were used for isolation of both GCs and SCs; all experiments during this isolation were performed at room temperature ($25\text{--}28^{\circ}\text{C}$).

For isolation of GCs, 1 g of MPGs was pretreated as described above and incubated in 100 mL of incubation solution (15% sucrose) in a Petri dish 15 cm in diameter with shaking at 75 rpm and 26°C in the dark. After incubation for 55–65 min when the germinated pollen grains had a pollen tube shorter than the long axis of the pollen grain, the germinated pollen grains were collected by use of a 300-mesh screen to remove the incubation solution and shriveled pollen grains and were immediately osmotically shocked in 100 mL isolation buffer (IB) (10 mM MES–KOH pH 6.0, 5 mM EDTA, 10 mM NaCl, 0.15 mM spermine, 0.5 mM spermidine, 0.5 mM PMSF, 1 mM DTT, 7.5% sucrose) with intermittent stirring for 5 min. This bursting mixture was sieved through a 400-mesh screen to remove pollen debris. GCs in the filtrate were collected by centrifugation at 500g for 5 min, then washed twice with IB. Collected GCs were purified by a Percoll density gradient (18% and 24% Percoll in IB) at 1000g for 20 min. GCs at the interface of 18% and 24% Percoll were collected by use of a glass pipet and washed twice with IB at 500g for 5 min. The purified GCs were snap-frozen in liquid nitrogen and stored at -80°C .

For isolation of SCs, 0.5 g of MPGs was pretreated as described above and cultured in 100 mL of germination medium (1.6 mM H_3BO_3 , 1 mM KCl, 0.5 mM CaCl_2 , 15% sucrose) modified according to Prado et al.²⁵ in a Petri dish 15 cm in diameter with shaking at 75 rpm and at 28°C in the dark. After incubation for 9.5–10 h, when GCs completed PMII to generate SCs in growing pollen tubes, the pollen tubes were collected by use of an 80-mesh screen to remove germination medium, ungerminated pollen grains, and pollen grains with short pollen tubes and were immediately transferred to 100 mL of 15% sucrose medium. After incubation for 10 min with intermittent stirring, pollen tubes were burst to release SCs. This bursting mixture was filtered through a 300-mesh screen to remove cell debris, and SCs in the filtrate were collected by centrifugation at 600g for 5 min and washed twice with IB. Resulting SCs were purified by a Percoll density gradient (8% and 13% Percoll in IB) with centrifugation at 1000g for 20 min. SCs at the interface of 8% and 13% Percoll were collected by use of a glass pipet and washed twice with IB at 600g for 5 min.

The purified SCs were snap-frozen in liquid nitrogen and stored at -80°C .

Microscopy Observation

Microscopy observation involved use of a Zeiss AXIO microscope (Zeiss, Germany). Cell integrity and morphologic features of isolated GCs and SCs were determined by acetocarmine staining (1% carmine in 45% glacial acetic acid).²⁶ Cell nuclei were visualized by 4',6-diamidino-2-phenylindole (DAPI) staining. For staining of GCs and SCs in germinated pollen grains and pollen tubes, pollen grains and tubes were transferred to DAPI staining solution (1 $\mu\text{g}/\text{mL}$ DAPI, 50% glycerol, 10 mM PBS, 25 $\mu\text{g}/\text{mL}$ 1,4-diazabicyclo[2.2.2]octane) and stained for at least 30 min in the dark. Isolated GCs and SCs were stained by directly applying DAPI staining solution to samples on slides. DAPI-stained cells were examined under UV-fluorescence in the DAPI channel.

Flow Cytometry Analysis

To determine the relative DNA contents of GC and SC nuclei, 1 g MPGs was washed with 15% sucrose to remove the lipid materials enclosing the pollen grain, then collected by use of a 300-mesh screen; pollen tubes that had completed PMII were collected as described in the Isolation of GCs and SCs section, above. These pretreated MPGs and pollen tubes were chopped by use of a sharp razor blade in a glass Petri dish 5.5 cm in diameter that contained 5 mL ice-cold chopping buffer (200 mM Tris-Cl, pH 7.5, 4 mM MgCl_2 , 0.1% (v/v) Triton X-100) on ice to release GC and SC nuclei, respectively. The resulting mixtures were filtered through a 400-mesh screen to remove cell debris and unbroken pollen grains. The filtrate was transferred to a new 1.5-mL centrifuge tube and supplemented with DAPI stock solution (1 $\mu\text{g}/\mu\text{L}$ in water) to a final content of 2 $\mu\text{g}/\text{mL}$. DAPI-stained nuclear samples were used immediately for flow cytometry. The nuclear fluorescence was measured by use of a MoFlo XDP high-speed flow cytometer (Beckman-Coulter, USA) with a 70- μm ceramic nozzle at 60 psi sheath pressure. DAPI fluorescence was excited with a UV laser (355-nm) and AlexaFluor 488 with an argon ion laser (488-nm) and detected with a 457-/50-nm HQ band-pass filter. The sheath solution was the chopping buffer described above.

Protein Sample Preparation

GCs and SCs stored in IB (about 5×10^4 and 8×10^4 cells, respectively) were diluted to 200 μL with ice-cold sonication buffer (20 mM Tris-Cl pH 8.5, 150 mM NaCl, 10 mM EDTA, 10 mM DTT, 1 mM PMSF, 1 \times protease inhibitor cocktail, Roche), respectively. Cells were lysed by use of the Vibra Cell VCX105 sonicator (Sonics & Materials) on ice at 30% amplitude with 10 s effective time (pulsed 5 s on, 5 s off), and this procedure was repeated six times with a 2-min break between two subsequent times. Cell lysates stained with acetocarmine were examined by microscopy. After all cells were completely broken, the lysate was supplemented with octyl β -D-glucopyranoside at a final content of 0.1% and then shaken at 220 rpm and 25°C for 20 min to better dissolve membrane proteins. Then, lysates were centrifuged at 12000g for 5 min to remove cell debris; the supernatant was transferred to a new 1.5-mL centrifuge tube and processed by use of the 2D Cleanup kit (GE Healthcare). Pelleted proteins were dissolved in 15–20 μL of protein lysis buffer (7 M urea, 2 M thiourea, 4% CHAPS, 20 mM Tris-Cl pH 8.5 for 2D-DIGE or 7 M urea, 2 M thiourea, 4% CHAPS, 40 mM DTT, 2% IPG buffer for

regular 2-DE) and centrifuged at 12000g and 4°C for 5 min to remove any debris. The supernatant was transferred to a new tube and stored at -80°C . Protein concentration was determined by the Bradford assay.²⁷ To evaluate efficiency of the protein preparation method, we examined protein samples by 12.5% SDS-PAGE and Coomassie Brilliant Blue G-250 staining according to Laemmli²⁸ and Candiano.²⁹ For 2D-DIGE analysis, three independent protein preparations from independent samples were separately produced for GCs and SCs.

2D-DIGE and Image Analysis

The pH of the protein sample was adjusted to 8.5, and 50 μg of proteins from the GC and SC samples were labeled with 400 pmol of Cy3 and Cy5 dyes, respectively. Proteins prepared by equally mixing the two samples were labeled with Cy2 as an internal standard. Labeling followed the manufacturer's protocol (CyDye DIGE Fluor, minimal labeling kit, 5 nmol; GE Healthcare). The labeled proteins and internal standard were mixed and diluted to 450 μL with rehydration buffer (7 M urea, 2 M thiourea, 2% CHAPS, 18 mM DTT, 0.5% 3–10 NL IPG buffer, 0.002% bromophenol blue). This mixture was cleaned by centrifugation at 20000g for 20 min at 25°C , then loaded onto a 24 cm 3–10 NL IPG strip (GE Healthcare). Isoelectric focusing involved a Multiphor II apparatus (GE Healthcare) in the dark at 20°C . The IPG strip was two-step-equilibrated, as described previously,³⁰ and the second-dimension separation was run on 12.5% polyacrylamide gels with an Ettan DALT SIX electrophoresis system (GE Healthcare) at 20°C by use of a constant-power mode at 2 W/gel for the first 45 min, then 7 W/gel to the end. The GC and SC protein samples were assigned to 3 DIGE gels representing three independent biological repeats of each of the GC and SC samples (Figure S1, Supporting Information).

Fluorescence images were acquired by use of a Typhoon 9400 fluorescent imager (GE Healthcare) at 488/520, 532/580, and 633/670 excitation/emission for Cy2, Cy3, and Cy5 images, respectively. This analysis generated nine images (3×3) with similar strength of total signal. The images were cropped by use of Image Quant TL 7.0 (GE Healthcare) to exclude unnecessary regions then imported into Decyder 6.5 (GE Healthcare). The biological variation analysis (BVA) module was used to analyze gel images and generate pick lists. Spots were automatically detected, matched, and normalized to the internal standard, then manually checked to guarantee correct matching across images. Spots reproducible in all nine images were used to identify differentially expressed protein (DEP) spots. Only proteins showing fold change in expression ≥ 1.2 with statistical significance (Student's *t* test 95%, $p \leq 0.05$) between GCs and SCs were considered to have significant change in expression.

Spectrometry Identification of Proteins

Protein spots were excised from gels as described previously.³¹ In-gel trypsin digestion was performed as described.³² MS/MS spectra were acquired on an ultrafleXtreme MALDI-TOF/TOF instrument (Bruker Daltonics). All spectra were obtained in positive ion reflectron mode under the control of flexControl 3.3. The matrix suppression was set to deflection, 500 Da. The spectra detection mass range was set at 700–4000 *m/z*. External calibration involved use of the Bruker Standard Peptide Calibration kit. For each spot, six peaks with the strongest intensity in MS spectra and a signal-to-noise threshold >30 were automatically selected as precursor ions

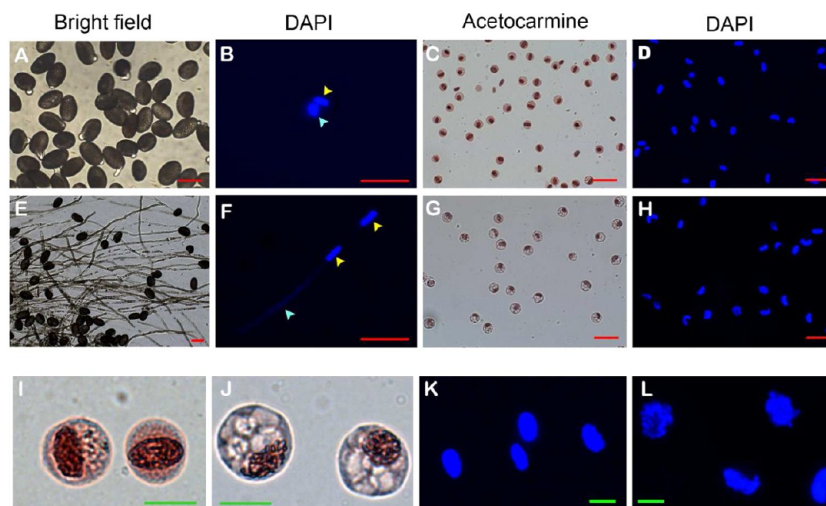


Figure 1. Cytological characterization of generative cells (GCs) and sperm cells (SCs) isolated from lily. (A, B) Just-germinated pollen grains (A) used for isolation of GCs and DAPI-labeled GC (yellow arrow) and vegetative cell (light green arrow) nucleus (B) in the just-germinated pollen grain. (C, D) Purified GCs examined by acetocarmine (C) and DAPI staining (D). (E, F) Pollen tubes cultured for 9.5 h used to isolate SCs (E) and DAPI-labeled SCs (yellow arrow) and vegetative cells (light green arrow) (F). (G, H) Purified SCs examined with acetocarmine (G) and DAPI staining (H). (I, J) Close-up of purified GCs (I) and SCs (J) stained with acetocarmine to show differences in cytoplasm. (K, L) Close-up of DAPI-stained GCs (K) and SCs (L) to show differences in nuclei. Red scale bar = 100 μm in A–H; green bar = 30 μm in I–L.

for MS/MS analysis. Flex Analysis 3.3 (Bruker Daltonics) was used for spectral processing and generating peak lists for both MS and MS/MS spectra. MS/MS peak lists were generated by use of a SNAP averaging algorithm with a signal-to-noise threshold >3 , and the calibration method for MS/MS spectra involved baseline subtraction (TopHat) and smoothing (Savitzky–Golay, width 0.15 m/z , cycles 4). Processed peak lists were submitted to the Mascot search engine (<http://www.matrixscience.com/>; Matrix Science, London, UK) via the biotool 3.2 interface (Bruker Daltonics) and searched against the NCBI nr protein database (<http://www.ncbi.nlm.nih.gov/>; Green plants, 1,084,913 sequences in NCBI 20120722). Searching parameters were taxonomy, viridiplantae (green plant); enzyme, trypsin; max missed cleavages, 1; fixed modification, carbamidomethylation (C); variable modification, oxidation (M); peptide mass tolerance, 100 ppm; MS/MS tolerance, 0.5 Da. Only significant hits determined by Mascot probability analysis with $p < 0.05$ were considered.

Data Mining and Bioinformatic Analysis

The function annotation of identified proteins was mainly retrieved from the NCBI protein database (<http://www.ncbi.nlm.nih.gov/>) and Uniprot (<http://www.uniprot.org/>). For proteins without clear function information, the function information was referred from conserved domains, which were searched by use of SMART (<http://smart.embl-heidelberg.de/>), Interpro (<http://www.ebi.ac.uk/interpro/>), and pfam (<http://pfam.sanger.ac.uk/>). Proteins were functionally categorized according to their molecular and biological functions. *Arabidopsis* homologues of inquired proteins were detected by use of TAIR BLAST 2.2.8 on the TAIR Web site (<http://www.Arabidopsis.org/>). Protein interaction network analysis involved use of the STRING 9.5 search tool (<http://string-db.org>) by referring to yeast homologues that were obtained by a WU-Blast search of the “PROTEIN ENCODING (S288C)” data set at the SGD Web site (<http://www.yeastgenome.org/>). A hit with the highest score at $p < 0.05$ and with the same molecular and biological function as the inquired protein was considered as a homologue.

Western Blot Analysis

Proteins from GCs and SCs were prepared as described above and separated by 12% SDS-PAGE. Proteins in a gel were electrophoretically transferred onto a PVDF membrane (Pierce, USA) with a transfer buffer containing 25 mM Tris, 192 mM glycine, and 20% methanol and then immunodetected as described previously.¹⁶ For each Western blot test, three biological repeats were performed. Signal intensities in Western blot bands were quantified by analyzing the membrane images with ImageJ (NIH, USA). These primary rabbit antibodies used were phosphoenolpyruvate carboxykinase (Beijing Protein Innovation no. DGW7, Beijing, China) and vacuolar invertase (Beijing Protein Innovation no. DGW3, Beijing, China) from *Oryza sativa*. All of these primary rabbit antibodies were used at a dilution of 1:1000.

RESULTS

Isolation and Characterization of GCs and SCs

Mature lily pollen is bicellular at anthesis, so PMII occurs in polarly growing pollen tubes to generate SCs. This feature allows isolating GCs and SCs in vitro on a large scale for “omics” study. In this study, we established a method to isolate and purify GCs from just-germinated pollen grains and SCs from growing pollen tubes in which PMII had been completed. To guarantee successful isolation of highly purified GCs and SCs, we optimized in vitro pollen-germination medium by modifying the medium popularly used for lily pollen.²⁵ We removed 2-(*N*-morpholino)ethanesulfonic acid (MES) and increased sucrose to a concentration of 15% because our data showed that pollen tubes in MES medium burst after culture for 4–5 h when PMII did not occur (data not shown). We also optimized the culture conditions, including temperature and shaking speed. Finally, we found that lily pollen tubes could grow stably for 10 h in this modified germination medium (for details, see Materials and Methods) at 28 °C in the dark with shaking at 75 rpm.

Furthermore, we determined the time when SCs were produced in growing pollen tubes by monitoring GCs and SCs

with DAPI staining. When incubated in the modified germination medium for about 1 h, pollen grains produced a tube shorter than the length of the pollen grain, and GCs did not move into the tube (Figure 1A, B). For about 7 h, most of the GCs in tubes began to divide, and nuclei of newly formed SCs appeared as elongated stick-shaped (data not shown). For about 9.5 h, more than 90% of the GCs in tubes completed division to generate SCs whose nuclei became short stick-shaped (Figure 1E, F). Therefore, we isolated and purified GCs from just-germinated pollen grains with short tubes and SCs from pollen tubes cultured for 9.5 h by osmosis shocking and gradient density centrifugation.

Microscopy observation revealed that this procedure greatly removed contamination of cell debris and cytoplasm materials and was highly efficient in enriching GCs and SCs. Purified GCs and SCs had intact cell structure (Figure 1C, D, G, H). Using this procedure, we could obtain 5×10^4 GCs or 8×10^4 SCs from 4 g of mature pollen grains. The isolated GCs and SCs were nearly spherical and of uniform size, with diameters of about 35 and 40 μm , respectively. However, they differed in cytoplasm and cell nuclear structure. SCs had many vacuole-like structures in the cytoplasm, which was rarely observed in the GCs (Figure 1I, J). Moreover, DAPI staining was weaker in SCs than in GCs (Figure 1K, L). Most GC nuclei were regular long-oval shaped, whereas SC nuclei were more random in shape, and only a few showed a regular oval shape. These nuclei appearances were considered to be associated with the chromatin structure and suggested that SCs had less condensed chromatin than GCs.

Cell Cycle Analysis of SCs

Studies have shown that SCs can initiate DNA replication before fertilization, and therefore, mature SCs may be at different cell cycle stages of G1 and G2 phases.⁴ To dissect the cell cycle control strategies of SCs, we analyzed the relative DNA content in the nuclei of the GCs and SCs. We prepared nuclear suspensions from mature pollen grains and pollen tubes growing in germination medium for 9.5 h by a blade chopping method (Figure 2A, B). Relative DNA content of the nuclear suspensions was measured by flow cytometry. Both samples showed a pair of peaks with about 2-fold change in relative DNA content (Figure 2C–F). Because Lanzhou lily is diploid ($2n = 2x = 24$)³³ and the vegetative nuclei of pollen are haploid, SCs, almost identical to GCs, were diploid and arrived at the G2 phase of cell cycle. Therefore, mature SCs showed completed DNA replication and stayed at the G2 phase of the cell cycle.

Protein Expression Profiles of GCs and SCs

GCs and SCs contain mainly nuclei, with little cytoplasm (Figure 1I, J). Our preliminary experiment demonstrated that these nuclei were somewhat resistant to urea lysis buffer and were difficult to lyse with commonly used lysis buffer. The highly enriched nucleic acids also interfered with protein separation in 2-DE gels. We found that ultrasonication could effectively disrupt the nuclei (Figure 3A). SDS-PAGE revealed that proteins prepared by ultrasonication contained nuclear proteins, such as core histones (Figure 3A). In addition, ultrasonication was efficient in shearing nucleic acids in these cells, thus eliminating interference of nuclear acids with protein separation on 2-DE.

To compare protein expression profiles of GCs and SCs and identify DEPs between the two distinct samples, we compared the resolution of 2D-DIGE with linear pH strips of 4–7 and 3–

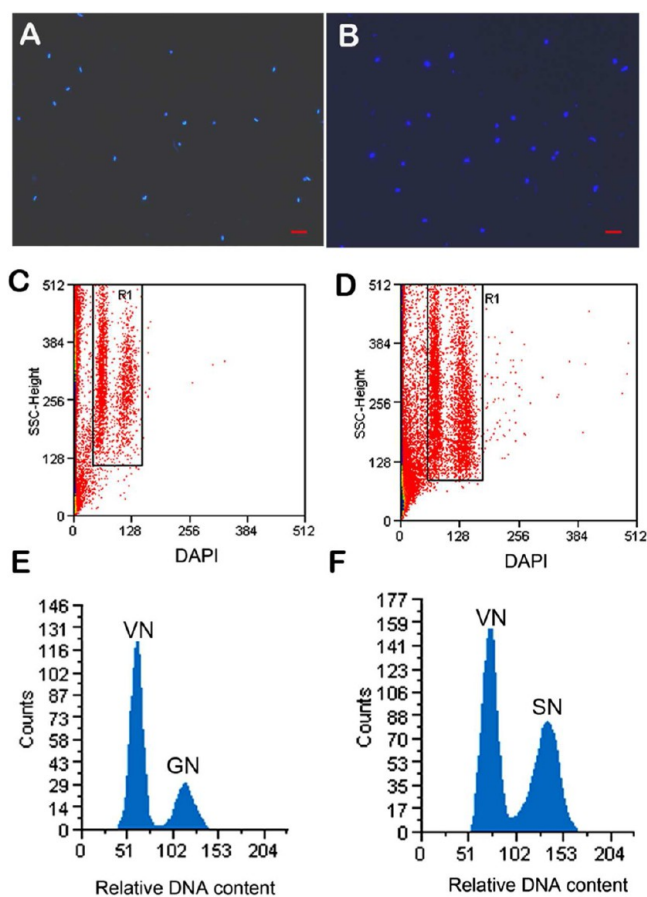


Figure 2. Flow cytometry of relative DNA content in GCs and SCs. (A, B) Nuclear suspension prepared from mature pollen grains (A) and pollen tubes cultured for 9.5 h (B). (C, D) Side scatter channel (SSC) versus DAPI plots of samples A (C) and B (D). (E, F) The gated regions in C and D plots correspond to the histograms in E and F, respectively. GN, generative cell nuclei; SN, sperm cell nuclei; VN, vegetative cell nuclei. Scale bar = 100 μm in A and B.

10 and with nonlinear pH gradient strips of 3–10 NL in separating these proteins. Strips with the 3–10 NL pH gradient showed better resolution than strips with the 4–7 and 3–10 line pH gradients (data not shown). Therefore, we analyzed protein expression profiles of GCs and SCs by 2D-DIGE with 3–10 NL pH gradient strips. The experiment was performed in triplicate biological repeats with reciprocal dye labels to ensure the reproducibility of protein patterns. We detected about 2500 protein spots in each image (representative image in Figure 3B; all images in Supporting Information Figure S1). GCs and SCs had similar protein expression profiles, with some spots showing significant changes in levels (Figure 3B). Spots reproducible in all images were used to identify DEP spots in the two distinct samples. Statistical analysis revealed 226 protein spots with significant changes in expression during SC development; for 124, the level was increased, and for 102, it was decreased in SCs.

Identification and Functional Categories of Differentially Expressed Proteins

Among 226 DEP spots, we successfully excised 128 from gels (Figure 3B) and obtained MS/MS spectra for the 128 spots by spectrometry. Because lily is unsequenced and comprehensive protein data for this plant are lacking, we searched these spectra against the NCBI green plant data set. This analysis led to

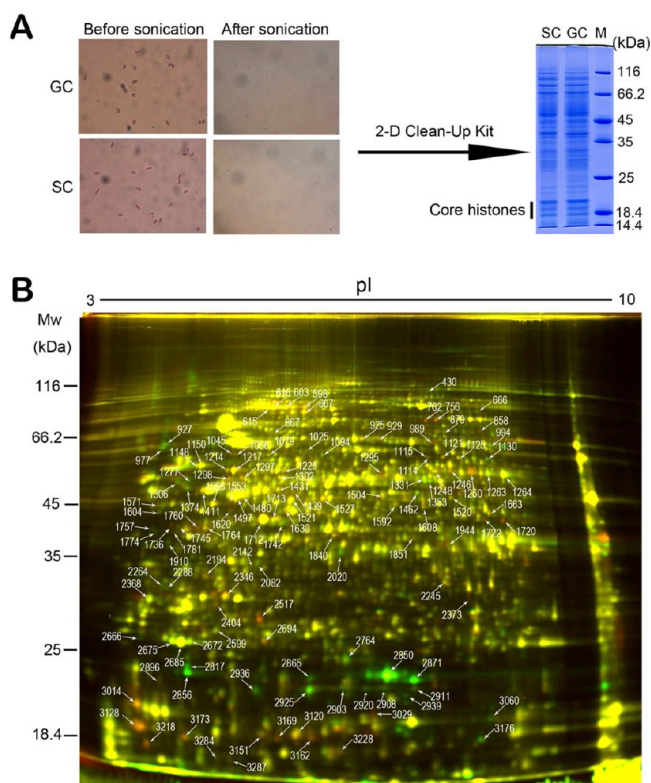


Figure 3. 2D Differential in-gel electrophoresis (2D-DIGE) of proteins from GCs and SCs. (A) GCs and SCs before and after sonication for protein preparation and SDS-PAGE examination of proteins from GCs and SCs. (B) Picked protein spots for mass spectrometry identification in a representative 2D-DIGE image. Proteins from GCs and SCs were labeled with Cy3 (green color channel), and Cy5 (red color channel), respectively. 2D-DIGE images were acquired by use of a Typhoon 9410 scanner. Differential expression of these protein spots was determined statistically (for details, see Materials and Methods). All images are shown in Supporting Information Figure S1, and information supporting protein identification are in Supporting Information Figure S2 and Tables S1–S2. Molecular mass (in kilodaltons) and pI of proteins are shown on the left and top of the image, respectively.

identification of 105 spots (Table 1; Tables S1 and S2, Supporting Information). Among them, 101 contained a single protein each (Table 1), and the other four had two proteins each (Table S2, Supporting Information). The remaining 23 spots could not be identified with the present database, although high-quality MS/MS spectra were obtained for these spots. Because it is impossible to determine whether each of the two proteins identified from one spot changed in abundance, therefore, our further analysis focused on the 101 identities, which represented 82 unique proteins (Tables 1; Table S1, Supporting Information).

To validate identities of proteins and their differential expression in GCs and SCs detected by 2D-DIGE-based proteomic approaches, we examined the expression profiles of two identified proteins (spots 879 and 2936, Table 1) using Western blot because of the availability of antibodies against them (Figure 4). The Western blot results showed that the two proteins were specifically detected and displayed obviously down-regulated expression in SCs, as compared with GCs (Figure 4), which were consistent with those detected by 2D-DIGE (Table 1). Thus, this indicated the reliability of 2D-DIGE-based proteomic results.

Furthermore, we annotated the 101 DEPs using the protein bioinformatics database (for details, see Materials and Methods). On the basis of molecular function and biological process, these DEPs were organized into 11 functional categories (Table 1). In all, 71% were involved in six main functional groups—metabolism (14%), the cell cycle (14%), signaling (13%), the ubiquitin/proteasome pathway (10%), chromatin remodeling (10%), and stress response (10%)—with the remaining 29% in another five groups (Table 1, Figure 5A). Proteins implicated in the cell cycle, chromatin remodeling, stress response, protein biosynthesis, and signaling had more isoforms than those in other groups (Figure 5B). Thus, these data suggested that signaling, the ubiquitin/proteasome pathway, chromatin remodeling, and cell-cycle control may contribute greatly to SC differentiation, and protein biosynthesis and stress response are relatively active in this process.

Expression pattern analysis revealed that most of the DEPs in 8 out of 11 groups were up-regulated in SCs; especially, those involved in the ubiquitin/proteasome pathway and cell cycle were almost all up-regulated (Figure 5C). In addition, some proteins implicated in the cell cycle and DNA repair were associated with the ubiquitin/proteasome pathway, such as SKP1 (spot 3128), CUL1 (spots 3162 and 3169), NPL4 (spot 1553), and DD11 (spot 1620), which showed up-regulated expression in SCs. In contrast, almost all proteins involved in chromatin remodeling (8/10) and stress response (8/10) were down-regulated in SCs (Figure 5C). Within the chromatin remodeling group, multicopy suppressor of Ira (MSI1-like) family proteins (spots 994, 1331, 1353 and 1374) are subunits of chromatin assembly factor 1 (CAF-1) complex, which consists of three proteins (FAS1, FAS2, and MSI1 in *Arabidopsis*).^{34,35} High mobility group (HMG) proteins (spots 2903, 2908, 2911, and 2920) belong to a class of chromosomal nonhistone proteins common in eukaryotes.³⁶

Among the down-regulated stress-response proteins (Table 1, Figure 5C), most were ripening and desiccation-inducible proteins, such as LEA (late embryogenesis abundant) and LLA23 proteins. LEA proteins were found to increase in level in seeds at the late development stage and are associated with tolerance to dehydration stress and cold shock.³⁷ They are also abundant in mature pollen.³⁸ LLA-23, characterized as a water-deficit/ripening-induced protein in lily pollen, accumulates only at the late stage of pollen maturation and presumably is associated with desiccation of mature pollen.³⁵ Correspondingly, overexpression of LLA-23 in *Arabidopsis* significantly increased drought resistance.⁴⁰ These proteins were highly expressed in GCs, but significantly down-regulated in SCs (Table 1). This observation may explain why mature lily bicellular pollen grains can endure long-term storage in vitro.

Biological Function of *Arabidopsis* Proteins Homologous to These Differentially Expressed Proteins

Numerous studies have functionally characterized many proteins (genes) from *Arabidopsis*. To examine the function information of these DEPs in plant reproductive development, we searched *Arabidopsis* proteins homologous to these DEPs (Table 1; Table S3, Supporting Information) and summarized known functions of the homologues from published results of mutant studies (Table 1; Table S3, Supporting Information). By homology searching, we found that 98 of the 101 DEPs mapped to *Arabidopsis* proteins and 43 of the 98 *Arabidopsis* proteins had mutant phenotypes reported. Among the

Table 1. Proteins with Differential Expression in Generative Cells and Sperm Cells of Lily

spot number	accession number	description	<i>t</i> test statistic ^a	fold change in expression (SC/GC)	yeast homologue ^b	<i>Arabidopsis</i> homologue ^c
Metabolism 14 (14) ^d						
666	gil152013366	β -galactosidase 14	6.01×10^{-03}	-1.49		BGAL14
867	gil8978290	oligopeptidase A	2.32×10^{-02}	1.5	PRD1	AT5G65620
879	gil220938674	phosphoenolpyruvate carboxykinase	1.38×10^{-02}	-1.6	PCK1	PCK1 ^S
929	gil75110834	UDP-sugar pyrophosphorylase	4.77×10^{-04}	1.34	QRI1	USP ^M
1121	gil209978716	galactokinase	2.50×10^{-04}	1.53	GAL1	GAL1
1248	gil356527314	mitochondrial-processing peptidase subunit β -like	1.49×10^{-03}	1.21	MAS1	MPPBETA
1431	gil114421	mitochondrial F1-ATPase beta subunit	5.11×10^{-03}	1.21	ATP2	AT5G08690
1592	gil603221	6-phosphogluconate dehydrogenase	5.70×10^{-03}	1.21	GND1	AT3G02360
1742	gil115874	serine carboxypeptidase 3	3.97×10^{-02}	-1.33	PRC1	SCPL48
1840	gil223947343	α -1,4-glucan-protein synthase	4.33×10^{-04}	1.4		RGPI/2 ^M
1851	gil357440383	isocitrate dehydrogenase (NAD+)	8.09×10^{-03}	1.53	IDH2	IDH-V
1944	gil120666	glyceraldehyde-3-phosphate dehydrogenase	2.94×10^{-02}	1.33	TDH2	GAPC1 ^M
2817	gil225425306	nudix hydrolase 13, mitochondrial-like	4.33×10^{-06}	-19	DDP1	ATNUDT13
2936	gil3219509	vacuolar invertase	3.17×10^{-02}	-4.05	SUC2	AT1G62660
Cell Cycle 14 (9)						
598	gil168046900	YT521-B-like domain containing protein	9.30×10^{-06}	1.55		ECT5
603	gil2492504	cell division cycle protein 48 homologue	3.76×10^{-04}	1.66	CDC48	CDC48A ^{EM}
615	gil2492504	cell division cycle protein 48 homologue	1.11×10^{-03}	1.53	CDC48	CDC48A ^{EM}
616	gil2492504	cell division cycle protein 48 homologue	1.08×10^{-03}	1.5	CDC48	CDC48A ^{EM}
667	gil168046900	YT521-B-like domain containing protein	1.56×10^{-04}	1.53		ECT5
1214	gil224100473	importin subunit α -1-like	1.21×10^{-03}	1.4	SRP1	IMPA-2
1217	gil224100473	importin subunit α -1-like	2.74×10^{-05}	1.53	SRP1	IMPA-2
1462	gil217073888	proliferation-associated protein 2G4	1.78×10^{-03}	-1.49	MAP2	EBP1 ^C
1553	gil326528657	nuclear pore localization protein NPL4	2.33×10^{-02}	1.44	NPL4	NPL41
1620	gil115444859	DNA-damage inducible protein DDI1-like	8.11×10^{-04}	1.56	DDI1	DDI1
2373	gil56785267	putative cyclin-dependent kinase B1-2	4.24×10^{-02}	1.63	CDC28	CDKB1;1 ^C
3128	gil241872560	pollen specific SKP1-like protein LSK1	3.63×10^{-05}	2.38	SKP1	SKP1 ^M
3162	gil241872566	CULLIN1-like protein 1	4.15×10^{-03}	1.86	CDC53	CUL1 ^E
3169	gil241872566	CULLIN1-like protein 1	6.88×10^{-03}	1.65	CDC53	CUL1 ^E
Signaling 13 (11)						
1025	gil82623395	GDP dissociation inhibitor 1-like	1.46×10^{-02}	1.22	GDI1	GDI1 ^R
1148	gil147805412	metallophosphatase superfamily protein	8.62×10^{-03}	-1.26		AT3G09970
1246	gil90655299	alkaline phytase isoform 2	1.01×10^{-03}	1.65		AT1G09870
1250	gil57900566	polynucleotide kinase 3 phosphatase	4.97×10^{-03}	2.22	TPP1	AT3G14890
1263	gil57900566	polynucleotide kinase 3 phosphatase	2.96×10^{-02}	-1.25	TPP1	AT3G14890
1264	gil57900566	polynucleotide kinase 3 phosphatase	8.89×10^{-03}	-1.28	TPP1	AT3G14890
1295	gil356543778	diacylglycerol kinase iota-like	2.71×10^{-03}	1.55		DGK5 ^S
1757	gil255073331	protein kinase superfamily protein	4.02×10^{-03}	-2.13	TOS3	STN8
2082	gil1346750	Ser/Thr-protein phosphatase PP1 isozyme 1	4.56×10^{-02}	-1.36	GLC7	TOPP3
2142	gil18394249	serine-threonine kinase receptor-associated protein	2.14×10^{-01}	-1.21		AT1G15470
2194	gil16433	protein phosphatase 1A	2.10×10^{-03}	1.23	GLC7	TOPP2
2404	gil1168191	14-3-3 protein 4	7.74×10^{-04}	1.68	BMH2	GRF7
2666	gil13194672	calmodulin-like protein	1.39×10^{-03}	-2.23	CMD1	CML42 ^T
Ubiquitin/Proteasome Pathway 10 (9)						
1115	gil3450889	19S proteasome subunit 9	3.33×10^{-02}	1.41	RPN6	RPN6
1226	gil29124136	ubiquitin activating enzyme (E1) subunit APPBP1	5.95×10^{-04}	1.43	ULA1	AXR1/AXL ^E
1504	gil224108954	26S proteasome non-ATPase regulatory subunit 11	9.38×10^{-03}	1.31	RPN6	RPN6
1566	gil556560	rice homologue of Tat binding protein	7.12×10^{-04}	1.3	RPT5	RPT5A ^M
1571	gil18396650	ubiquitin thioesterase otubain-like protein	3.30×10^{-03}	1.66		AT1G28120
1608	gil192912954	26S proteasome subunit RPN5b	5.49×10^{-05}	1.43	RPN5	RPN5B ^M
1630	gil2952433	putative ubiquitin activating enzyme E1	1.76×10^{-03}	1.27	UBA3	ECRI ^V
1760	gil3641314	COP9 signalosome complex subunit CSN5	8.92×10^{-03}	1.37	RR1	CSNSA ^C
1764	gil3641314	COP9 signalosome complex subunit CSN5	2.27×10^{-02}	1.21	RR1	CSNSA ^C
2245	gil15237785	26S proteasome non-ATPase regulatory subunit 14	1.19×10^{-02}	1.3	RPN11	AT5G23540

Table 1. continued

spot number	accession number	description	<i>t</i> test statistic ^a	fold change in expression (S/GC)	yeast homologue ^b	<i>Arabidopsis</i> homologue ^c
Chromatin Remodeling 10 (7)						
994	gil2599092	WD-40 repeat protein MSI4	4.15×10^{-04}	-1.91	MSI1	MSI4 ^F
1331	gil2599092	WD-40 repeat protein MSI4	6.99×10^{-04}	-1.6	MSI1	MSI4 ^F
1353	gil332806931	FVE/MSI4, subunit C of CAF1 complex	2.68×10^{-03}	-1.57	HAT2	MSI4 ^F
1374	gil167593879	MSI1, multicopy suppressor of Ira1	1.08×10^{-03}	-1.48	HAT2	MSI1 ^{M,E,F}
1722	gil326533568	SANT DNA-binding domain containing protein	1.02×10^{-02}	2.27		KAN4 ^O
2903	gil194466163	high mobility group protein 1	1.06×10^{-02}	-1.69	NHP6A	HMGB2 ^S
2908	gil194466163	high mobility group protein 1	9.09×10^{-03}	-1.78	NHP6A	HMGB2 ^S
2911	gil194466163	high mobility group protein 1	2.64×10^{-03}	-1.62	NHP6A	HMGB2 ^S
2920	gil118488125	HMG-box superfamily of DNA-binding proteins	6.60×10^{-03}	-2.63	NHP6A	HMGB3
3014	gil145350142	SAM-dependent methyltransferases	1.23×10^{-03}	1.75		AT4G33110
Stress Response 10 (6)						
1045	gil356526803	probable nucleoredoxin 1-like	8.20×10^{-03}	1.66		AT1G60420 ^M
1056	gil356526803	probable nucleoredoxin 1-like	3.84×10^{-03}	1.92		AT1G60420 ^M
2672	gil21322750	LEA-like protein	2.10×10^{-04}	-1.62		AT4G36600
2675	gil21322750	LEA-like protein	4.90×10^{-04}	-1.62		AT4G36600
2685	gil21322750	LEA-like protein	1.21×10^{-04}	-1.47		AT4G36600
2850	gil6525055	pollen-specific desiccation-associated LLA23	6.38×10^{-08}	-11.24		
2856	gil356513299	PMRSN domain containing SGNH ₁ hydrolase	3.08×10^{-06}	-16.83		TBL23
2871	gil6525055	pollen-specific desiccation-associated LLA23	3.02×10^{-06}	-15.26		
2925	gil544437	phospholipid hydroperoxide glutathione peroxidase	1.30×10^{-03}	-3.46	GPX2	ATGPX6
2939	gil90265065	peptide methionine sulfoxide reductase	3.60×10^{-03}	-5.18	MXR1	PMSR1 ^S
Protein Biosynthesis 8 (6)						
925	gil108709561	lysyl-tRNA synthetase	1.09×10^{-03}	1.23	KRS1	ATKRS-1
1094	gil115436616	asparaginyl-tRNA synthetase	1.12×10^{-02}	-1.33	SLM5	SYNC1 ^E
1439	gil303844	eukaryotic initiation factor 4A	4.34×10^{-02}	1.85	TIF2	EIF4A1
1521	gil303844	eukaryotic initiation factor 4A	1.48×10^{-03}	1.35	TIF2	EIF4A1
2368	gil6015064	elongation factor 1-delta	2.56×10^{-03}	-1.4	EFB1	AT1G30230 ^V
3029	gil8778393	eukaryotic translation initiation factor 5A	5.81×10^{-03}	1.99	ANB1	ELF5A-1 ^V
3151	gil8778393	eukaryotic translation initiation factor 5A	1.91×10^{-02}	1.39	ANB1	ELF5A-1 ^V
3228	gil118482257	40S ribosomal protein S12	3.63×10^{-05}	1.44	RPS12	AT2G32060
RNA Binding 6 (6)						
858	gil225464938	heterogeneous nuclear ribonucleoprotein Q-like	2.90×10^{-03}	2.51	PAB1	AT3G52660
1079	gil115447237	lupus La protein family protein	3.94×10^{-02}	-1.22	LHP1	AtLa1 ^E
1297	gil194702946	RNA-binding (RRM/RBD/RNP motifs) family protein	1.22×10^{-04}	1.78	NAM8	RBP45B
1302	gil116787223	RNA-binding KH domain-containing protein	4.80×10^{-02}	1.34	PBP2	FLK ^F
1520	gil4680340	putative nucleolysin	3.07×10^{-02}	1.22	PUB1	UBP1B
1663	gil115438550	heterogeneous nuclear ribonucleoprotein A2/B1-like	3.66×10^{-03}	1.21	HRP1	UBA2c ^S
Cytoskeleton 6 (6)						
430	gil31339056	actin filament bundling protein P-115-ABP	2.49×10^{-02}	-1.81		VLN4 ^R
1411	gil303842	β -tubulin	7.63×10^{-04}	1.29	TUB2	TUB5
1480	gil135398	tubulin α -1 chain	3.42×10^{-03}	1.2	TUB1	TUA6 ^V
1497	gil6094431	α -3-tubulin	2.73×10^{-03}	1.3	TUB1	TUA5
1712	gil20329	actin	1.46×10^{-05}	1.27	ACT1	ACT7 ^V
1713	gil323650493	actin 7	5.27×10^{-03}	1.22	ACT1	ACT12
Protein Folding 4 (4)						
989	gil90657661	TCP-1/cpn60 chaperonin family protein	2.19×10^{-02}	1.54	CCT6	AT3G02530
1306	gil51090427	putative FKBP12 interacting protein	4.77×10^{-03}	-1.4		FIP37 ^E
2896	gil225433902	peptidyl-prolyl <i>cis-trans</i> isomerase E	3.78×10^{-04}	1.65		ATE1
3120	gil313510857	heat shock protein Hsp18.3	1.23×10^{-03}	1.36	HSP26	HSP18.2
Others 6 (4)						
1277	gil224145935	VHS domain containing protein	6.75×10^{-04}	-1.8	GGA1	AT5G16880
1736	gil115469064	zinc finger, RING-type domain containing protein	1.10×10^{-03}	1.88		AT5G08139
1745	gil115469064	zinc finger, RING-type domain containing protein	1.32×10^{-02}	-1.27		AT5G08139

Table 1. continued

spot number	accession number	description	<i>t</i> test statistic ^a	fold change in expression (SC/GC)	yeast homologue ^b	<i>Arabidopsis</i> homologue ^c
			Others 6 (4)			
1781	gil115469064	zinc finger, RING-type domain containing protein	1.34×10^{-02}	1.42		AT5G08139
2764	gil115456892	protein of unknown function DUF827	4.64×10^{-02}	-1.71		AT3G51220
3284	gil222622854	hypothetical protein Osj_06722	7.99×10^{-04}	1.35		

^a*t* Test indicates significant differences in expression of these proteins between GCs and SCs ($p < 0.05$). ^bYeast homologues of identified proteins were obtained by a WU-Blast search of the "Protein Encoding (S288c)" data set at the SGD Web site (<http://www.yeastgenome.org/>). A hit with the highest score at $p < 0.05$ and with the same molecular and biological function as the inquired protein was considered as a homologue; for details, see Supporting Information Table S4. ^c*Arabidopsis* homologues of identified proteins were obtained by a Blast search at the Tair Web site (www.arabidopsis.org); hits with the highest score and almost the same as highest score at $p < 0.05$ and with the same molecular and biological function as the inquired protein were considered as homologue. The reported mutant phenotypes of each homologue are labeled with a superscript after the protein name or locus number; the mutant defects are abbreviated as the following: M, male gametophyte; E, embryo; F, flowering time; O, ovule; S, stress response; V, vegetative growth; C, cell cycle; R, root hair; T, trichome branching. For details, see Supporting Information Table S3. ^dThe numbers following the protein category name indicate the number of total and unique proteins (in parentheses) in this category.

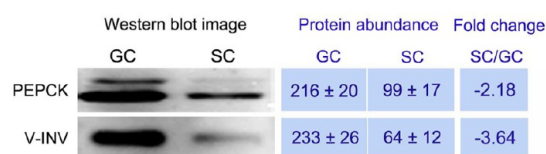


Figure 4. Western blot analysis of proteins. Proteins from GCs and SCs were separated by SDS-PAGE (10 μ g of proteins loaded for each lane) and transferred to PVDF membranes and, finally, immunodetected with primary rabbit antibodies against phosphoenolpyruvate-carboxykinase (PEPCK, 1:1000 dilution) and vacuolar invertase (V-INV, 1:1000 dilution). Signal intensities representing estimated protein abundances in Western blot bands were quantified with ImageJ. The quantified values are mean \pm SD ($\times 1000$) of three biological repeats. Fold change in expression (SC/GC) were calculated with the mean values of three biological repeats.

functionally known 43 proteins, more than one-half are involved in reproductive development, including pollen, embryo, ovule, and flowering time (Figure 6). Strikingly, the largest number of these proteins implicated in reproductive development are associated with pollen, and the second largest, with the embryo. These results clearly indicate the importance of these identified DEPs in male gamete formation and postfertilization embryo development.

Protein Interaction Network Analysis

To evaluate the biological function of DEPs, we analyzed their interaction network using yeast homologues and the online STRING 9.5 tool because current databases do not have enough information to support network analysis of proteins from plants, including *Arabidopsis*. For this analysis, we first determined 56 unique budding yeast (*Saccharomyces cerevisiae*) homologues from the 101 DEPs (Table 1; Table S4, Supporting Information) and submitted the 56 yeast proteins to a database search for network analysis. At a high confidence level (score > 0.7) with only experimental evidence considered, we revealed an interaction network for 25 of the 56 proteins (Figure 7).

This network could be divided into seven modules (Figure 7). Among the seven modules, three were associated with the SKP1, Cullin1/CDC53 and F-box (SCF) E3-ligase-mediated ubiquitin/proteasome pathway, DDI-mediated DNA damage response, and GTPase signaling (Figure 7) (to conveniently describe this result, here, we use only the name of yeast proteins; please refer to identified DEPs in Table 1). The first module contained Cullin1/CDC53 and SKP1, components of

the SCF complex,⁴¹ RRI1, component of the COP9 signalosome complex,⁴² and GDP dissociation inhibitor (GDI). The second module contained RPN6, RPN11, RPT5, and RPN5; components of the 19S proteasome regulatory particle of 26S proteasome;⁴³ and DDI1. DDI1 is an UBL-UBA domain-containing protein and is implicated in DNA damage response. The third module contained ULA1 and UBA3, which are involved in RUB1 conjugation and deconjugation to and from CDC53/Cullin1 together with COP9 signalosome.^{44,45} The circulatory RUB1 conjugation to CDC53/Cullins is essential for optimal activity of SCF complex and has been found to have a vital role in cell cycle control and embryogenesis in animals.⁴⁶

Two cell cycle modules involve CDC48, NPL4, KRS1, and PRC1 in one module and CDC28 and SRP1 in another (Figure 7). Among the remaining two, one involves RNA binding (NAM8, PAB1, PBP2), and one is functionally unclear (ACT1, CMD1, GLC7, and BMH2) (Figure 6). This analysis revealed the interaction among SCF-mediated proteolysis, the COP9 signalosome complex, GTPase signaling, cell cycle control, and DDI1-mediated DNA damage response in the GCs and SCs, which suggested that this proteolysis pathway may incorporate signals to build an expressway to selectively destruct proteins for SC development and function specification.

DISCUSSION

In this study, we have established a method to obtain highly purified GCs and SCs from just-germinated pollen grains and growing pollen tubes, respectively. Using this method, we could obtain a large amount of GCs and SCs suitable for proteomic analysis. 2D-DIGE-based proteomic analysis detected at least 2500 reproducible protein spots in each sample. Proteome comparison of the GCs and SCs revealed that among about 5000 protein spots in the two samples, 226 spots showed changes in levels, which suggests that sperm development from GCs is not associated with a significant change in proteome profiles. This notion appears to be supported by data that the transcriptional profile of lily GCs significantly overlapped with that of maize SCs.⁴⁷ Further spectrometry identification and functional category analysis revealed that the identified differentially expressed proteins were organized into 11 functional categories: 71% were involved in six main functional groups—metabolism, the cell cycle, signaling, the ubiquitin/proteasome pathway, chromatin remodeling, and stress response (Table 1, Figure 5A). Thus, sperm development

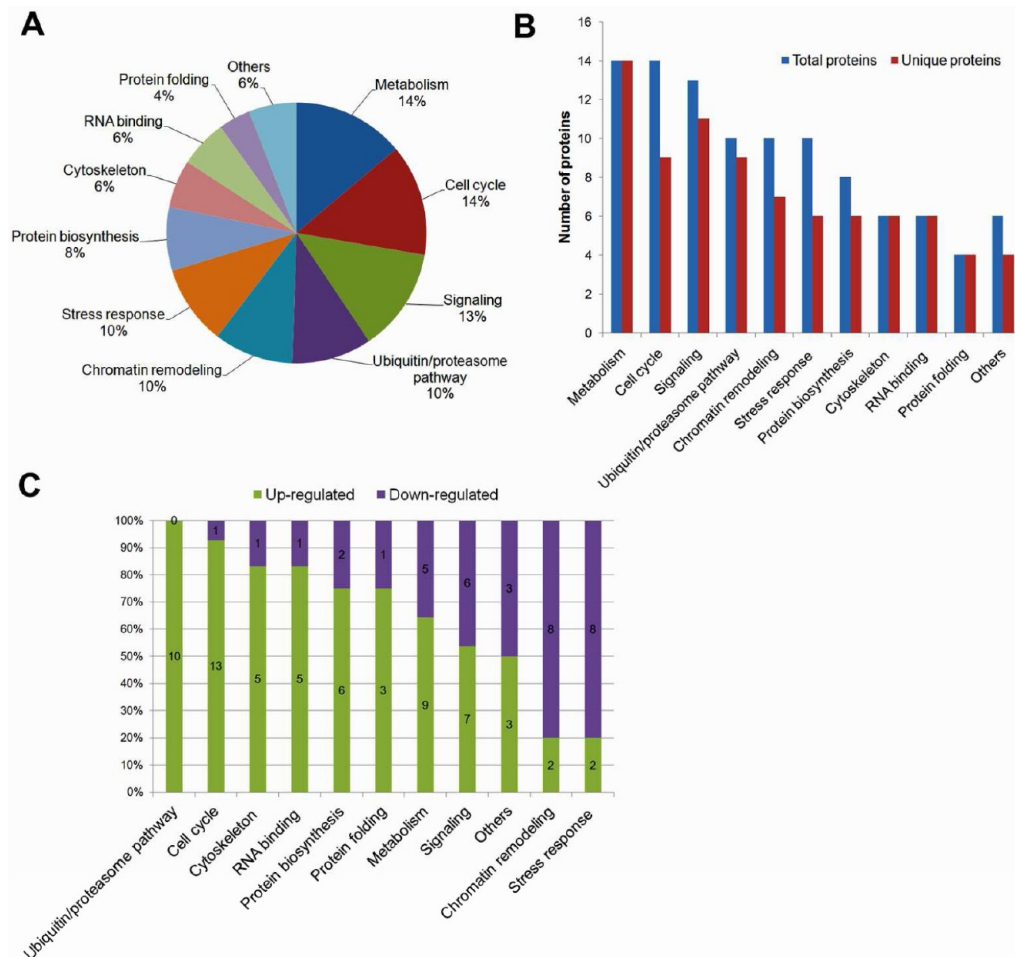


Figure 5. Functional categories of proteins differentially expressed in SCs as compared with GCs. (A) Percentage of proteins in each functional category. (B) Number of total proteins and unique proteins in each category. (C) Number and percentage of up- and down-regulated proteins in SCs in each functional category. Each bar of the histogram is labeled with the number of proteins.

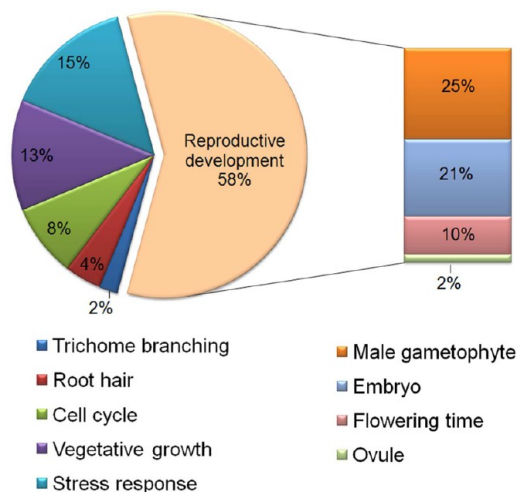


Figure 6. Mutant phenotypes of *Arabidopsis* homologues of differentially expressed proteins. Number in each sector represents the percentage of proteins in each phenotype class. Detailed information is in Supporting Information Table S3.

and function specification may involve fine-tuned changes in cellular and metabolism processes.

Several studies have revealed that genes involved in ubiquitin-mediated proteolysis were overrepresented in the SC transcriptome of rice and *Arabidopsis*^{11,12} and in expressed sequence tags of lily GCs.^{47,48} This implied that the proteolysis pathway may be important in the development of GCs to SCs and SC function specification. Our comparison of GC and SC proteomes showed that proteins related to this pathway were overrepresented in the DEP data set and that all these proteins were up-regulated in SCs (Table 1). The proteins represented the main components of the SCF E3-ligase-mediated ubiquitin/proteasome proteolysis system (Table 1, Figure 7). The SCF E3 ligase complex is known to control cell cycle progression, signaling, DNA damage repair, and genome stabilization by regulating the periodically selective degradation of regulators in these processes.^{49–51} For example, loss-of-function mutation in *FBL17* encoding an F-box protein that recognizes cell-cycle proteins KRP6/7 caused defect in PMII, and thus, the mutant generated bicellular pollen at anthesis in *Arabidopsis*.^{52,53}

Our data also showed that proteins (RR1/CSNS, spots 1760 and 1764; ULA1/AXR1, spot 1226; UBA3/ECR1, spot 1630) involved in RUB1 conjugation and deconjugation (also called neddylation and deneddylation) of Cullin1 were up-regulated in SCs. RUB1 conjugation and deconjugation may be important to regulate activity and substrate recognition of the SCF complex. In mice, the *uba3* mutant was defective in

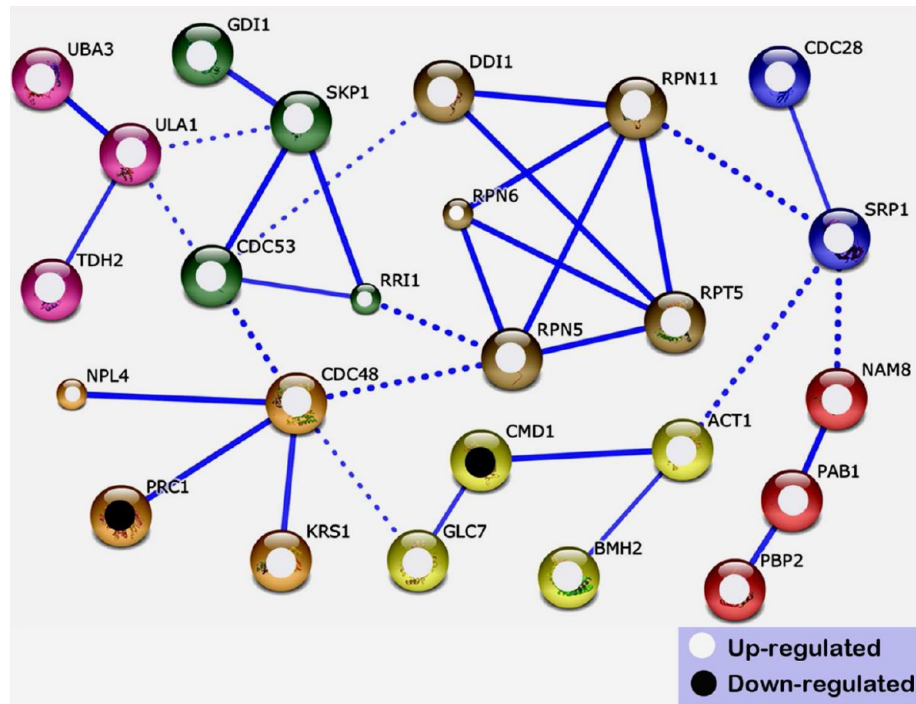


Figure 7. Protein interaction network analysis of differentially expressed proteins with yeast homologue proteins. Protein interactions at high confidence (score > 0.7) with only experimental evidence are considered, and protein nodes with no interaction and only scattered interaction are not displayed. Proteins in the interaction network are clustered into seven functional modules represented by different node colors. The interactions are indicated by a solid line (inner group) and a dashed line (between groups). Up- and down-regulated proteins in SCs are indicated with white and black spots centered in each node, respectively.

neddlylation and showed abnormal embryo development, cell cycle arrest, and accumulation of the SCF E3-ligase substrate cyclin E.⁵⁴ Cell cycle regulator CDC48 can bind only to neddylation SCF E3-ligase.⁵⁵ Furthermore, our network analysis revealed that the SCF E3-ligase-mediated ubiquitin/proteasome proteolysis pathway displayed interaction with the cell cycle, DNA damage response, and GTPase signaling (Figure 7). These lines of evidence clearly indicate that SCF E3-ligase-mediated proteolysis may be an important mechanism underlying SC development and function specification.

SC development from GC undergoes a strict mechanism for cell cycle control. This mechanism allows PMII progression of GCs to produce SCs. The newly “born” SCs undergo DNA replication and then are arrested in the cell cycle to prevent genome aneuploid. The resulting mature SCs stay at the G1 or G2 phase before fertilization.⁴ In accordance with this early observation, our results showed that SCs generated from GCs in polarly growing tubes were at the G2 phase (Figure 2). Studies have functionally characterized several genes essential for PMII progression in *Arabidopsis*, including *CDKA;1* and *DUO1/2*, encoding cell cycle protein CDKA;1 and R2R3 MYB transcription factor, respectively.^{6,8,56} However, this mechanism is not fully understood. Our data showed that cell-cycle-related proteins represented a main function category in the DEP data set, and this category contained important cell cycle regulators, such as CDKB1/CDC28 (spot 2373), CDC48 (spots 603, 615 and 616), and NPL4 (spot 1553) (Table 1). Almost all (13/14) of these identified cell-cycle-related proteins showed higher expression in SCs than in GCs, which implies enhanced control of the cell cycle in SCs. CDKB1 belongs to plant-specific B-type CDK.⁵⁷ *Arabidopsis* CDKB1;1 was required for the G2-to-M progression in stomatal precursor cells of cotyledons and was

also highly expressed in mature guard cells, which was terminally differentiated and exited the cell cycle.⁵⁸ Therefore, CDKBs may have roles in maintaining cells at a certain cell-cycle phase for several specific types of cells.

In the cell cycle module, CDKB1/CDC28 showed interaction with SRP1/importin- α (Figure 7). SRP1/importin- α is a classic nuclear localization signal receptor and is implicated in cell cycle progression via mediating transportation of proteins to nuclear.^{59,60} In animal cells, SRP1/importin- α -mediated nuclear protein import is cell-cycle-dependent.⁶¹ Increased expression of CDKB1/CDC28 and SRP1/importin- α in SCs suggests their involvement in SC cell cycle control. CDC48 and NPL4 are involved in cell cycle control via the functionally known CDC48/P97-UFD1-NPL4 complex. This complex is required for S-phase replication in embryonic cells and mitotic germ cells of adult worms.^{62,63} Up-regulated expression of CDC48 and NPL4 in SCs suggested that they may affect SC cell-cycle progression by controlling DNA replication. Together, these results suggest that plant-specific B-type CDK and CDC48-NPL4 pathways, along with coordination with SCF-mediated proteolysis, are important components underlying cell-cycle progression for SC development.

Genome integrity is essential for SCs to accurately transmit genetic information. Maintenance of genome integrity in germline cells involves chromatin condensation and an exact DNA repair mechanism. Compact chromatin condensation is a unique feature of male germline cells in both flowering plants and mammals. Such a high level of chromatin condensation is assumed to help optimize the nucleus shape and, hence, facilitate sperm transport to the embryo sac and to confer genome protection against the effects of genotoxic factors in mammals.⁶⁴ Deficiency in chromatin compaction in mammal

sperm leads to increased frequency of sperm DNA damage.⁶⁵ The chromatin condensation in mammal spermiogenesis is achieved by sequential replacement of somatic histones by testis-specific variants of histones, transitional proteins and protamines.^{66,67} In plants, no such ordered mechanism is reported in germline cell development. Only several histone variants and modifications are identified in lily and *Arabidopsis* pollen, including H2A, H2B, and abundant H3 variants, which are all expressed in germline cell nuclei but not in vegetative nuclei of pollen.^{5,23,68,69}

The mechanism underlying chromatin remodeling from GCs to SCs is largely unknown. Our cytological observations showed that chromatin was more condensed in GCs than in SCs (Figure 1K, L). Consistent with this observation, all identified chromatin-remodeling-related proteins, including MSI4/FVE (spots 994, 1331, and 1353), MSI1 (spot 1374), and HMG (spots 2865, 2903, 1908, 2911, and 2920), showed higher expression in GCs than in SCs (Table 1). MSI4 and MSI1 belong to MSI1-like family proteins, which are subunits of the CAF-1 complex.³⁴ This complex acts as a histone chaperone in chromatin assembly.^{34,70} MSI1-like proteins are essential for maintaining heterochromatin at a constitutively inactive state in plant reproductive development.^{35,71} HMG proteins belong to a class of chromosomal nonhistone proteins common in eukaryotes that participate in chromatin architecture remodeling by binding DNA.³⁶ MSI1 is required for GC division⁷² and MSI4 (FVE) for epigenetic repression of flowering locus C expression in *Arabidopsis*.⁷³ Knockout mutation of HMGs in mouse led to defective spermatogenesis.⁷⁴ Together with findings that these proteins have different expression levels in GCs and SCs (see above), these lines of evidence suggest that these proteins may contribute to chromatin packaging of GCs and SCs to the condensed state and to maintaining GC chromatin at an available state for PMII.

Our data showed that the DDII-mediated DNA damage response pathway was closely interacted with the SCF-mediated proteolysis pathway in the predicted network (Figure 7). DDI was initially identified in the DNA damage response⁷⁵ and is found to have roles in regulating the turnover of Ho endonuclease, a DSB inducer, via transferring ubiquitylated Ho to the 19S regulatory particle of the proteasome.^{76–78} Interestingly, the protein is also required for turnover of Ufo1, an F-box protein, which recruits Ho to the ubiquitination proteolysis pathway.^{76,78,79} The stage-specific degradation of Ufo1 and Ho is essential to cell cycle progression.^{76,79} The yeast double mutant of DD11 and RAD23 displayed cell cycle G2/M phase arrest at high temperature.⁸⁰ Together, these pieces of evidence suggest the importance of the coordination of DNA repair and cell-cycle progression in SC development and the involvement of the SCF E3-ligase-mediated ubiquitin/proteasome pathway in this coordination.

In summary, we established a pollen-tube culture condition that allows pollen tubes to grow for as long as 10 h in vitro when mature SCs are generated from GCs via PMII. Under this condition, we developed a method to isolate lily GCs and SCs from just-germinated pollen grains and growing pollen tubes via osmosis shocking. This method can generate a large amount of GCs and SCs at high purity, which allowed for the first comparative proteomic analysis of plant GCs and SCs. Our 2D-DIGE proteomic analysis screened 226 protein spots differentially expressed in GCs and SCs. These identified proteins are involved in diverse functional categories, with preference in metabolism, the cell cycle, signaling the SCF E3-ligase-

mediated ubiquitin/proteasome pathway, and chromatin remodeling. Furthermore, we revealed the importance of the coordination among SCF E3-ligase-mediated proteolysis, the cell cycle and DNA repair in SC development and function specification. This study revealed the comprehensive and dynamic features of the protein profiles of GCs and SCs.

■ ASSOCIATED CONTENT

📄 Supporting Information

(Figure S1) Experiment designs for CyDye label and 2D-DIGE gel images. (Figure S2) MS/MS spectra supporting protein identification based on a single confident peptide. (Table S1) Differentially expressed proteins identified by MALDI-TOF/TOF. (Table S2) Protein spots with multiple proteins identified in a single spot. (Table S3) *Arabidopsis* homologues of differentially expressed proteins and their mutant phenotypes. (Table S4) Yeast homologues of differentially expressed proteins used for the interaction network. This material is available free of charge via the Internet at <http://pubs.acs.org>.

■ AUTHOR INFORMATION

Corresponding Author

*Phone: +86-10-62836210. Fax: +86-10-62594170. E-mail: twang@ibcas.ac.cn.

Notes

The authors declare no competing financial interest.

■ ACKNOWLEDGMENTS

This work was supported by the Chinese Ministry of Science and Technology (Grant No. 2012CB910504) and the National Natural Science Foundation of China (Grant No. 31121065).

■ REFERENCES

- (1) McCormick, S. Male gametophyte development. *Plant Cell* **1993**, *5* (10), 1265–1275.
- (2) Borg, M.; Brownfield, L.; Twell, D. Male gametophyte development: a molecular perspective. *J. Exp. Bot.* **2009**, *60* (5), 1465–1478.
- (3) Singh, M. B.; Bhalla, P. L. Control of male germ-cell development in flowering plants. *Bioessays* **2007**, *29* (11), 1124–1132.
- (4) Friedman, W. E. Expression of the cell cycle in sperm of *Arabidopsis*: implications for understanding patterns of gametogenesis and fertilization in plants and other eukaryotes. *Development* **1999**, *126* (5), 1065–1075.
- (5) Okada, T.; Singh, M. B.; Bhalla, P. L. Histone H3 variants in male gametic cells of lily and H3 methylation in mature pollen. *Plant Mol. Biol.* **2006**, *62* (4), 503–512.
- (6) Iwakawa, H.; Shinmyo, A.; Sekine, M. *Arabidopsis CDKA1*, a *cdc2* homologue, controls proliferation of generative cells in male gametogenesis. *Plant J.* **2006**, *45* (5), 819–831.
- (7) Gusti, A.; Baumberger, N.; Nowack, M.; Pusch, S.; Eisler, H.; Potuschak, T.; De Veylder, L.; Schnittger, A.; Genschik, P. The *Arabidopsis thaliana* F-box protein FBL17 is essential for progression through the second mitosis during pollen development. *PLoS One* **2009**, *4* (3), e4780.
- (8) Durberry, A.; Vizir, I.; Twell, D. Male germ line development in *Arabidopsis*. duo pollen mutants reveal gametophytic regulators of generative cell cycle progression. *Plant Physiol.* **2005**, *137* (1), 297–307.
- (9) Alandete-Saez, M.; Ron, M.; Leiboff, S.; McCormick, S. *Arabidopsis thaliana* GEX1 has dual functions in gametophyte development and early embryogenesis. *Plant J.* **2011**, *68* (4), 620–632.
- (10) von Besser, K.; Frank, A. C.; Johnson, M. A.; Preuss, D. *Arabidopsis HAP2 (GCS1)* is a sperm-specific gene required for pollen

tube guidance and fertilization. *Development* **2006**, *133* (23), 4761–4769.

(11) Borges, F.; Gomes, G.; Gardner, R.; Moreno, N.; McCormick, S.; Feijó, J. A.; Becker, J. D. Comparative transcriptomics of *Arabidopsis* sperm cells. *Plant Physiol.* **2008**, *148* (2), 1168–1181.

(12) Russell, S. D.; Gou, X.; Wong, C. E.; Wang, X.; Yuan, T.; Wei, X.; Bhalla, P. L.; Singh, M. B. Genomic profiling of rice sperm cell transcripts reveals conserved and distinct elements in the flowering plant male germ lineage. *New Phytol.* **2012**, *195* (3), 560–573.

(13) Slotkin, R. K.; Vaughn, M.; Borges, F.; Tanurdžić, M.; Becker, J. D.; Feijó, J. A.; Martienssen, R. A. Epigenetic reprogramming and small RNA silencing of transposable elements in pollen. *Cell* **2009**, *136* (3), 461–472.

(14) Pertl, H.; Schulze, W. X.; Obermeyer, G. The pollen organelle membrane proteome reveals highly spatial–temporal dynamics during germination and tube growth of lily pollen. *J. Proteome Res.* **2009**, *8* (11), 5142–5152.

(15) Holmes-Davis, R.; Tanaka, C. K.; Vensel, W. H.; Hurkman, W. J.; McCormick, S. Proteome mapping of mature pollen of *Arabidopsis thaliana*. *Proteomics* **2005**, *5* (18), 4864–4884.

(16) Dai, S.; Li, L.; Chen, T.; Chong, K.; Xue, Y.; Wang, T. Proteomic analyses of *Oryza sativa* mature pollen reveal novel proteins associated with pollen germination and tube growth. *Proteomics* **2006**, *6* (8), 2504–2529.

(17) Wu, X.; Chen, T.; Zheng, M.; Chen, Y.; Teng, N.; Šamaj, J.; Baluška, F. e.; Lin, J. Integrative proteomic and cytological analysis of the effects of extracellular Ca²⁺ influx on *Pinus bungeana* pollen tube development. *J. Proteome Res.* **2008**, *7* (10), 4299–4312.

(18) Dai, S.; Wang, T.; Yan, X.; Chen, S. Proteomics of pollen development and germination. *J. Proteome Res.* **2007**, *6* (12), 4556–4563.

(19) Kost, B. Spatial control of Rho (Rac-Rop) signaling in tip-growing plant cells. *Trends Cell Biol* **2008**, *18* (3), 119–127.

(20) Singh, M. B.; Bhalla, P. L.; Russell, S. D. Molecular repertoire of flowering plant male germ cells. *Sex. Plant Reprod.* **2008**, *21* (1), 27–36.

(21) Xu, H.; Swoboda, I.; Bhalla, P. L.; Singh, M. B. Male gametic cell-specific gene expression in flowering plants. *Proc. Natl. Acad. Sci. U.S.A.* **1999**, *96* (5), 2554–2558.

(22) Mori, T.; Kuroiwa, H.; Higashiyama, T.; Kuroiwa, T. GENERATIVE CELL SPECIFIC 1 is essential for angiosperm fertilization. *Nat. Cell Biol.* **2005**, *8* (1), 64–71.

(23) Xu, H.; Swoboda, I.; Bhalla, P. L.; Singh, M. B. Male gametic cell-specific expression of H2A and H3 histone genes. *Plant Mol. Biol.* **1999**, *39* (3), 607–614.

(24) Okada, T.; Singh, M. B.; Bhalla, P. L. Histone H3 variants in male gametic cells of lily and H3 methylation in mature pollen. *Plant Mol. Biol.* **2006**, *62* (4–5), 503–512.

(25) Prado, A. M.; Porterfield, D. M.; Feijó, J. A. Nitric oxide is involved in growth regulation and re-orientation of pollen tubes. *Development* **2004**, *131* (11), 2707–2714.

(26) Jahier, J. *Techniques of Plant Cytogenetics*; Science Pub Inc: Lebanon, NH, 1996.

(27) Bradford, M. M. A rapid and sensitive method for the quantitation of microgram quantities of protein utilizing the principle of protein-dye binding. *Anal. Biochem.* **1976**, *72* (1–2), 248–254.

(28) Laemmli, U. K. Cleavage of structural proteins during the assembly of the head of bacteriophage T4. *Nature* **1970**, *227* (5259), 680–685.

(29) Candiano, G.; Bruschi, M.; Musante, L.; Santucci, L.; Ghiggeri, G. M.; Carnemolla, B.; Orecchia, P.; Zardi, L.; Righetti, P. G. Blue silver: a very sensitive colloidal Coomassie G-250 staining for proteome analysis. *Electrophoresis* **2004**, *25* (9), 1327–1333.

(30) Lau, A. T. Y.; Chiu, J. F. Proteomic and biochemical analyses of in vitro carcinogen-induced lung cell transformation: Synergism between arsenic and benzo[*a*]pyrene. *Proteomics* **2006**, *6* (5), 1619–1630.

(31) Xu, S. B.; Yu, H. T.; Yan, L. F.; Wang, T. Integrated proteomic and cytological study of rice endosperms at the storage phase. *J. Proteome Res.* **2010**, *9* (10), 4906–4918.

(32) Shevchenko, A.; Henrik Tomas, J. H.; Olsen, J. V.; Mann, M. In-gel digestion for mass spectrometric characterization of proteins and proteomes. *Nat. Protoc.* **2007**, *1* (6), 2856–2860.

(33) Zhang, S.; Ren, Y.; Liu, D.; Li, J. Karyotypic comparison between wild lilies and cultivated lilies. *J. Agric. Univ. Hebei* **2010**, *33* (4), 38–42.

(34) Hennig, L.; Bouveret, R.; Grussem, W. MSII-like proteins: an escort service for chromatin assembly and remodeling complexes. *Trends Cell Biol.* **2005**, *15* (6), 295–302.

(35) Hennig, L.; Taranto, P.; Walser, M.; Schönrock, N.; Grussem, W. *Arabidopsis* MSII is required for epigenetic maintenance of reproductive development. *Development* **2003**, *130* (12), 2555–2565.

(36) Grasser, M.; Lentz, A.; Lichota, J.; Merkle, T.; Grasser, K. D. The *Arabidopsis* genome encodes structurally and functionally diverse HMGB-type proteins. *J. Mol. Biol.* **2006**, *358* (3), 654–664.

(37) Goyal, K.; Walton, L. J.; Tunnaclyffe, A. LEA proteins prevent protein aggregation due to water stress. *Biochem. J.* **2005**, *15* (388 (Pt 1)), 151–157.

(38) Wolkers, W. F.; McCready, S.; Brandt, W. F.; Lindsey, G. G.; Hoekstra, F. A. Isolation and characterization of a D-7 LEA protein from pollen that stabilizes glasses in vitro. *Biochim. Biophys. Acta* **2001**, *1544* (1–2), 196–206.

(39) Wang, C.-S.; Liao, Y.-E.; Huang, J.-C.; Wu, T.-D.; Su, C.-C.; Lin, C. H. Characterization of a desiccation-related protein in lily pollen during development and stress. *Plant Cell Physiol.* **1998**, *39* (12), 1307–1314.

(40) Yang, C. Y.; Chen, Y. C.; Jauh, G. Y.; Wang, C. S. A lily ASR protein involves abscisic acid signaling and confers drought and salt resistance in *Arabidopsis*. *Plant Physiol.* **2005**, *139* (2), 836–846.

(41) Deshaies, R. SCF and Cullin/Ring H2-based ubiquitin ligases. *Annu. Rev. Cell. Dev. Biol.* **1999**, *15* (1), 435–467.

(42) Dohmann, E. M. N.; Levesque, M. P.; De Veylder, L.; Reichardt, I.; Jürgens, G.; Schmid, M.; Schwechheimer, C. The *Arabidopsis* COP9 signalosome is essential for G2 phase progression and genomic stability. *Development* **2008**, *135* (11), 2013–2022.

(43) Smalle, J.; Vierstra, R. D. The ubiquitin 26S proteasome proteolytic pathway. *Annu. Rev. Plant Biol.* **2004**, *55*, 555–590.

(44) Liakopoulos, D.; Doenges, G.; Matuschewski, K.; Jentsch, S. A novel protein modification pathway related to the ubiquitin system. *EMBO J.* **1998**, *17* (8), 2208–2214.

(45) Cope, G. A.; Suh, G. S. B.; Aravind, L.; Schwarz, S. E.; Zipursky, S. L.; Koonin, E. V.; Deshaies, R. J. Role of predicted metalloprotease motif of Jab1/Csn5 in cleavage of Nedd8 from Cull1. *Science* **2002**, *298* (5593), 608.

(46) Pan, Z. Q.; Kentsis, A.; Dias, D. C.; Yamoah, K.; Wu, K. Nedd8 on cullin: building an expressway to protein destruction. *Oncogene* **2004**, *23* (11), 1985–1997.

(47) Okada, T.; Bhalla, P. L.; Singh, M. B. Expressed sequence tag analysis of *Lilium longiflorum* generative cells. *Plant Cell Physiol.* **2006**, *47* (6), 698–705.

(48) Okada, T.; Singh, M. B.; Bhalla, P. L. Transcriptome profiling of *Lilium longiflorum* generative cells by cDNA microarray. *Plant Cell Rep.* **2007**, *26* (7), 1045–1052.

(49) Ang, X. L.; Harper, J. W. SCF-mediated protein degradation and cell cycle control. *Oncogene* **2005**, *24* (17), 2860–2870.

(50) Reed, S. I. Ratchets and clocks: the cell cycle, ubiquitylation and protein turnover. *Nat. Rev. Mol. Cell Biol.* **2003**, *4* (11), 855–864.

(51) Silverman, J. S.; Skaar, J. R.; Pagano, M. SCF ubiquitin ligases in the maintenance of genome stability. *Trends Biochem. Sci.* **2011**, *37* (2), 66–73.

(52) Liu, J.; Zhang, Y.; Qin, G.; Tsuge, T.; Sakaguchi, N.; Luo, G.; Sun, K.; Shi, D.; Aki, S.; Zheng, N. Targeted degradation of the cyclin-dependent kinase inhibitor ICK4/KRP6 by RING-type E3 ligases is essential for mitotic cell cycle progression during *Arabidopsis* gametogenesis. *Plant Cell* **2008**, *20* (6), 1538–1554.

- (53) Kim, H. J.; Oh, S. A.; Brownfield, L.; Hong, S. H.; Ryu, H.; Hwang, I.; Twell, D.; Nam, H. G. Control of plant germline proliferation by SCF^{FBL17} degradation of cell cycle inhibitors. *Nature* **2008**, *455* (7216), 1134–1137.
- (54) Tateishi, K.; Omata, M.; Tanaka, K.; Chiba, T. The NEDD8 system is essential for cell cycle progression and morphogenetic pathway in mice. *J. Cell Biol.* **2001**, *155* (4), 571.
- (55) den Besten, W.; Verma, R.; Kleiger, G.; Oania, R. S.; Deshaies, R. J. NEDD8 links cullin-RING ubiquitin ligase function to the p97 pathway. *Nat. Struct. Mol. Biol.* **2012**, *19* (5), 511–516.
- (56) Rotman, N.; Durbarry, A.; Wardle, A.; Yang, W. C.; Chaboud, A.; Faure, J. E.; Berger, F.; Twell, D. A novel class of MYB factors controls sperm-cell formation in plants. *Curr. Biol.* **2005**, *15* (3), 244–248.
- (57) Vandepoele, K.; Raes, J.; De Veylder, L.; Rouzé, P.; Rombauts, S.; Inzé, D. Genome-wide analysis of core cell cycle genes in *Arabidopsis*. *Plant Cell* **2002**, *14* (4), 903–916.
- (58) Boudolf, V.; Barrôco, R.; de Almeida Engler, J.; Verkest, A.; Beeckman, T.; Naudts, M.; Inzé, D.; De Veylder, L. B1-type cyclin-dependent kinases are essential for the formation of stomatal complexes in *Arabidopsis thaliana*. *Plant Cell* **2004**, *16* (4), 945–955.
- (59) Pulliam, K. F.; Fasken, M. B.; McLane, L. M.; Pulliam, J. V.; Corbett, A. H. The classical nuclear localization signal receptor, importin- α , is required for efficient transition through the G1/S stage of the cell cycle in *Saccharomyces cerevisiae*. *Genetics* **2009**, *181* (1), 105–118.
- (60) Loeb, J.; Schlenstedt, G.; Pellman, D.; Kornitzer, D.; Silver, P. A.; Fink, G. R. The yeast nuclear import receptor is required for mitosis. *Proc. Natl. Acad. Sci. U.S.A.* **1995**, *92* (17), 7647–7651.
- (61) Yasuhara, N.; Takeda, E.; Inoue, H.; Kotera, I.; Yoneda, Y. Importin α/β -mediated nuclear protein import is regulated in a cell cycle-dependent manner. *Exp. Cell Res.* **2004**, *297* (1), 285–293.
- (62) Mouyset, J.; Deichsel, A.; Moser, S.; Hoegel, C.; Hyman, A. A.; Gartner, A.; Hoppe, T. Cell cycle progression requires the CDC-48^{UFD-1/NPL-4} complex for efficient DNA replication. *Proc. Natl. Acad. Sci. U.S.A.* **2008**, *105* (35), 12879–12884.
- (63) Franz, A.; Orth, M.; Pirson, P. A.; Sonnevile, R.; Blow, J. J.; Gartner, A.; Stemmann, O.; Hoppe, T. CDC-48/p97 coordinates CDT-1 degradation with GINS chromatin dissociation to ensure faithful DNA replication. *Mol. Cell* **2011**, *44* (1), 85–96.
- (64) Miller, D.; Brinkworth, M.; Iles, D. Paternal DNA packaging in spermatozoa: more than the sum of its parts? DNA, histones, protamines and epigenetics. *Reproduction* **2010**, *139* (2), 287–301.
- (65) Cho, C.; Jung-Ha, H.; Willis, W. D.; Goulding, E. H.; Stein, P.; Xu, Z.; Schultz, R. M.; Hecht, N. B.; Eddy, E. M. Protamine 2 deficiency leads to sperm DNA damage and embryo death in mice. *Biol. Reprod.* **2003**, *69* (1), 211–217.
- (66) Ausió, J.; Brewer, L. R.; Frehlick, L. Genome organization by vertebrate sperm nuclear basic proteins (SNBPs). *Epigenetics and Human Reproduction*; Springer Press: New York, 2011, 213–230.
- (67) Kimmins, S.; Sassone-Corsi, P. Chromatin remodelling and epigenetic features of germ cells. *Nature* **2005**, *434* (7033), 583–589.
- (68) Okada, T.; Endo, M.; Singh, M. B.; Bhalla, P. L. Analysis of the histone H3 gene family in *Arabidopsis* and identification of the male-gamete-specific variant AtMGH3. *Plant J.* **2005**, *44* (4), 557–568.
- (69) Ueda, K.; Kinoshita, Y.; Xu, Z. J.; Ide, N.; Ono, M.; Akahori, Y.; Tanaka, I.; Inoue, M. Unusual core histones specifically expressed in male gametic cells of *Lilium longiflorum*. *Chromosoma* **2000**, *108* (8), 491–500.
- (70) van Nocker, S. CAF-1 and MSI1-related proteins: linking nucleosome assembly with epigenetics. *Trends Plant Sci.* **2003**, *8* (10), 471–473.
- (71) Pazhouhandeh, M.; Molinier, J.; Berr, A.; Genschik, P. MSI4/FVE interacts with CUL4–DDB1 and a PRC2-like complex to control epigenetic regulation of flowering time in *Arabidopsis*. *Proc. Natl. Acad. Sci. U.S.A.* **2011**, *108* (8), 3430–3435.
- (72) Chen, Z.; Tan, J. L. H.; Ingouff, M.; Sundaresan, V.; Berger, F. Chromatin assembly factor 1 regulates the cell cycle but not cell fate during male gametogenesis in *Arabidopsis thaliana*. *Development* **2008**, *135* (1), 65–73.
- (73) Ausín, I.; Alonso-Blanco, C.; Jarillo, J. A.; Ruiz-García, L.; Martínez-Zapater, J. M. Regulation of flowering time by FVE, a retinoblastoma-associated protein. *Nat. Genet.* **2004**, *36* (2), 162–166.
- (74) Hock, R.; Furusawa, T.; Ueda, T.; Bustin, M. HMG chromosomal proteins in development and disease. *Trends Cell Biol.* **2007**, *17* (2), 72–79.
- (75) Liu, Y.; Xiao, W. Bidirectional regulation of two DNA-damage-inducible genes, MAG1 and DD11, from *Saccharomyces cerevisiae*. *Mol. Microbiol.* **1997**, *23* (4), 777–789.
- (76) Ivantsiv, Y.; Kaplun, L.; Tzirkin-Goldin, R.; Shabek, N.; Raveh, D. Unique role for the Ubl-Uba protein Ddi1 in turnover of SCF^{Ufo1} complexes. *Mol. Cell Biol.* **2006**, *26* (5), 1579–1588.
- (77) Kaplun, L.; Tzirkin, R.; Bakhrat, A.; Shabek, N.; Ivantsiv, Y.; Raveh, D. The DNA damage-inducible Ubl–Uba protein Ddi1 participates in Mec1-mediated degradation of Ho endonuclease. *Mol. Cell Biol.* **2005**, *25* (13), 5355–5362.
- (78) Voloshin, O.; Bakhrat, A.; Herrmann, S.; Raveh, D. Transfer of Ho endonuclease and Ufo1 to the proteasome by the Ubl–Uba shuttle protein, Ddi1, analysed by complex formation in vitro. *PLoS One* **2012**, *7* (7), e39210.
- (79) Kaplun, L.; Ivantsiv, Y.; Bakhrat, A.; Tzirkin, R.; Baranes, K.; Shabek, N.; Raveh, D. The F-box protein, Ufo1, maintains genome stability by recruiting the yeast mating switch endonuclease, Ho, for rapid proteasome degradation. *Isr. Med. Assoc. J.* **2006**, *8* (4), 246–248.
- (80) Diaz-Martínez, L. A.; Kang, Y.; Walters, K. J.; Clarke, D. J. Yeast UBL–UBA proteins have partially redundant functions in cell cycle control. *Cell Div.* **2006**, *1*, 28.